Feasibility Study and Sensitivity Analysis for a Reconfigurable Dual Reflector Antenna

Cecilia Cappellin[1], Knud Pontoppidan[2]

TICRA, Læderstræde 34, 1201 Copenhagen, Denmark

[1]cc@ticra.com

[2]kp@ticra.com

***Abstract*— A feasibility study of a shaped dual reflector antenna equipped with a reconfigurable subreflector for a realistic mission scenario in Ku band is presented. The reconfigurable surface will be modelled by a mesh of interwoven flexible wires, supported by control points. A detailed sensitivity analysis to actuator settings will be performed.**

I. Introduction

The increased in orbit lifetime of today's telecommunication satellites combined with the rapid development of the offered services require always more flexible payloads. In this context, the existence of antennas that can be reconfigured in orbit and thus accommodate future service scenarios has recently attracted the interest of the international community. The benefits of such antennas are several: allowing the use of the same spacecraft at several orbital locations, changing the coverages during the satellite lifetime, and compensating for varying weather conditions. Shaped reflectors lack so far the capability of being reconfigurable in orbit, while this is possible with an array-fed parabolic reflector.

Several examples of possible reconfigurable shaped reflectors were studied over the years [1]-[3]. Though important and fundamental conclusions could be drawn from them, these past investigations have dealt with single offset reflectors and simple theoretical coverages. There was a need to consider a realistic mission scenario and antenna configuration, in order to clarify the benefits that could be achieved in real life.

The purpose of the present work is to study and quantify the properties, advantages and limitations provided by a shaped dual reflector equipped with a reconfigurable subreflector when applied to a realistic mission scenario in Ku band. Mechanical pointing and a fixed shape of the main reflector will be assumed. The reconfigurable surface will be modelled by a mesh of interwoven flexible wires with circular cross section, supported by a number of control points and with a free rim. While the fundamental properties of the flexible wire mesh with actuators have been described in previous articles [3], we will here concentrate on the benefits on the antenna performances provided by a reconfigurable subreflector. A sensitivity analysis to the actuator settings will then be performed. The effect on the antenna minimum gain of a random error uniformly distributed and added to the actuators *z*-coordinates will be considered. Specific actuator failures will be finally taken into account and the possibility of reshaping the surface to compensate for the actuator failure will be evaluated.

The paper is organized as follows: Section II and Section III describe the mission scenario and the antenna optical system, respectively; Section IV summarizes the benefits provided by the use of a reconfigurable subreflector while sensitivity analysis results for the reconfigurable surface technology are contained in Section V.

The study was performed in 2008 within the framework of an ARTES 1 project with ESA, under the contract 21306/07/NL/CLP "Flexible reflector antennas in the context of European Telecommunications strategy - A feasibility study".

II. Mission Scenario

The scenario under investigation is the so-called Intercontinental mission suggested by Thales Alenia Space (TAS). It is constituted by three coverages, one over Central Africa (B_1+B_2), one over South Africa (C_1+C_2+C_3), and one over Russia (D_1+D_2), see Fig. 1.

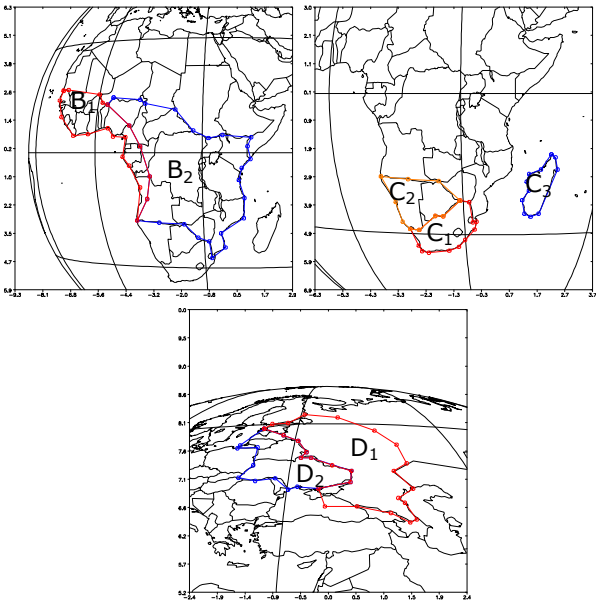

Fig. 1 Polygons B_1, B_2, C_1, C_2 and C_3 and D_1 and D_2 seen from 36E.

The coverages are illuminated by a geostationary satellite which can be located between 10E and 70E. The directivity required over the coverages is given in TABLE I, where "Ref"

means the maximum possible directivity for each coverage. A minimum XPD of 30 dB and a beam pointing error of 0.12° are considered, while no isolation constraints are expected. The antenna works in Tx/Rx in the frequency bands Tx=10.95-12.50 GHz and Rx=13.75-14.5 GHz. In general, reconfigurability is foreseen 18 times in the satellite life time (approximately once a year) and is required both in varying the satellite orbital location and in switching from one coverage to another.

TABLE I
DIRECTIVITY REQUIREMENTS FOR THE COVERAGES UNDER INVESTIGATION

Polygon and antenna directivity	Polygon and antenna directivity	Polygon and antenna directivity
B_1 Ref_B	C_1 Ref_C	D_1 Ref_D
B_2 Ref_B - 4 dB	C_2 Ref_C - 1 dB	D_2 Ref_D - 4 dB
	C_3 Ref_C - 7 dB	

III. ANTENNA OPTICAL SYSTEM

A dual offset Gregorian reflector antenna designed by Thales is mounted on the spacecraft lateral side and generates all coverages. The main reflector consists of a paraboloid with circular projected aperture of diameter D = 2.4 m, see Fig. 2. The subreflector is an ellipsoid with circular projected aperture D_2 = 0.8 m. The Mizuguchi condition for cross polarization cancellation is applied.

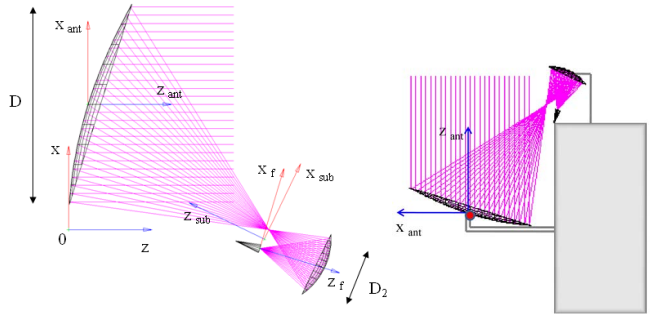

Fig. 2 Dual reflector geometry (on the left) and antenna mounted on the satellite lateral side with the RPM indicated (on the right).

The feed is linearly polarized along x_f and y_f, where $x_f y_f z_f$ is the feed coordinate system (CS), with origin at the second focal point of the ellipsoid, z_f pointing towards the center of the subreflector and x_f lying on the xz-plane. It is described by a Spherical Wave Expansion at the frequencies of interest. The antenna CS is defined by x_{ant} y_{ant} $z_{ant,}$ parallel to the xyz-CS and with origin at the center point of the main reflector surface. A reflector pointing mechanism (RPM) is assumed at the center of the main reflector.

IV. FEASIBILITY RESULTS

With the purpose of limiting the number of optimizations but at the same time investigating the largest number of parameters, a single orbital location (36E) was considered. Five frequencies (10.95, 11.7, 12.5, 13.75 and 14.5 GHz) and only one polarization (x_f) of the feed were taken into account.

The satellite CS $x_s y_s z_s$ is defined with origin at the satellite location, x_s-axis towards West, y_s-axis towards North and z_s-axis pointing towards the sub-satellite point on the Earth, see Fig. 3. The coverages are written in the satellite CS and the approximate center of each coverage is (u_i,v_i) with i =1,2,3. The antenna, which shall only provide service to one coverage at the time, is mounted on the satellite lateral side in such a way that the antenna CS points towards the approximate center of gravity (u_g,v_g) of all the coverages. While the feed and the subreflector are fixed in this position, the main reflector is equipped with an RPM by which it is tilted towards the midpoint between (u_g,v_g) and (u_i,v_i), depending on the coverage the antenna has to generate, to make the field radiated by the dual reflector antenna pointing towards (u_i,v_i). Far-field results and coverage polygons will be expressed in the satellite CS. Three different cases are analysed. In all of them, the optimization is performed with the software POS5 [4] with the well-established spline modelling or with the actuator and interwoven mesh technology, in order to satisfy the requirements on directivity and XPD on the coverages.

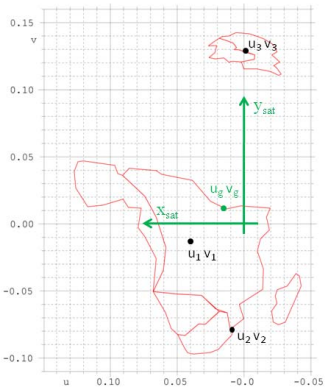

Fig. 3 Polygon coverages in the satellite CS and their centers (u_i,v_i) and the center of gravity (u_g,v_g) highlighted.

Case 1: Shaped subreflector and shaped main reflector for each individual coverage

The main reflector equipped by RPM and the subreflector are both shaped for each individual coverage, providing the best possible design for a shaped dual reflector optimized for each coverage. These results will be used as reference.

Case 2: Ellipsoidal subreflector and fixed main reflector shaped for all coverages

A traditional fixed main reflector shaped to maximize at the same time the minimum directivity on all the coverages is then analyzed. This represents the best and only possible solution when reconfigurability of the antenna cannot be achieved.

Case 3: Reconfigurable subreflector and shaped fixed main reflector

A shaped but fixed main reflector and a reconfigurable subreflector, optimized for each individual coverage, are finally investigated. The main reflector is fixed and shaped to provide, in case of ellipsoidal subreflector, a beam over the

Earth given by a circle of radius 0.1 in the *uv*-coordinate system. This is considered a good general main reflector which can be used when the coverages to be illuminated are not predefined but are free to assume arbitrary shapes during the satellite lifetime. The subreflector is reconfigurable and shaped by a mesh of interwoven wires controlled by 55 actuators, placed on a triangular grid with a spacing of 10 cm, see Fig. 4.

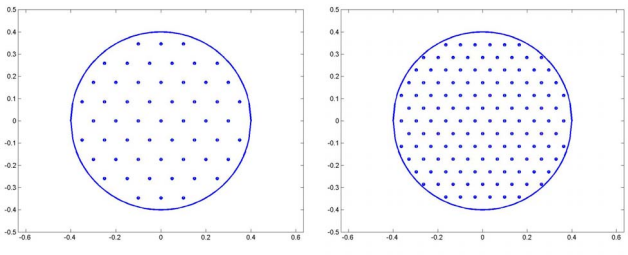

Fig. 4 Position of the actuators over the subreflector projected aperture: on the left 55 actuators, on the right 130 actuators.

On the basis of the main reflector size and the convergence mechanism, 30x30 and 12x12 splines are sufficient to shape the main reflector and the subreflector, respectively, for Case 1 and 2. Directivity levels obtained for Case 1 are reported in TABLE II. A summary of the directivity results computed for every case and relative to Case 1 is given in TABLE III.

TABLE II
DIRECTIVITY OBTAINED FOR CASE 1: 30X30 SPLINES ON THE MAIN REFLECTOR AND 12X12 SPLINES ON THE SUBREFLECTOR FOR EACH INDIVIDUAL COVERAGE

Polygon and antenna directivity		Polygon and antenna directivity		Polygon and antenna directivity	
B_1	30.9 dBi	C_1	34.5 dBi	D_1	36.1 dBi
B_2	26.9 dBi	C_2	33.5 dBi	D_2	32.1 dBi
		C_3	27.5 dBi		

TABLE III
DIRECTIVITY OBTAINED FOR CASE 1. CASE 2 AND CASE 3 RELATIVE TO CASE 1

	B_1	C_1	D_1
Case 1	30.9 dBi	34.5 dBi	36.1 dBi
Case 2	-2.9 dBi	-4.0 dBi	-4.1 dBi
Case 3	-1.9 dBi	-1.4 dBi	-1.2 dBi

The amplitude of the co-polar component of the far-fields over the coverage $C_1+C_2+C_3$ obtained by the different cases is shown in Fig. 5. It is seen that contour levels agree very well with the desired regions for Case 1, get definitely worse for Case 2 and significantly improve for Case 3.

From TABLE III it is observed that the difference relative to the best performances of Case 1 can be largely reduced when Case 3 is adopted. The improvement in directivity given by Case 3 with respect to the traditional performances of Case 2 is particularly evident for the smaller coverages ($C_1+C_2+C_3$ and D_1+D_2), where up to 2.9 dB can be gained, while it reduces for the largest coverage B_1+B_2.

It was found that directivity levels obtained by using N_i actuators can be equivalently obtained by splines over the reconfigurable surface if the number of splines along the *x*- and *y*- directions is chosen according to $N_{splines} \approx \text{sqrt}(2N_i)$. In the present case, 12x12 splines over the subreflector provide the same directivity results given by 55 actuators.

The subreflector shaping of Case 3 relative to the parent ellipsoid in the subreflector CS is shown in Fig. 6 for the coverage $C_1+C_2+C_3$. It was seen that the *z*-coordinates of the actuators relative to the parent ellipsoid lie in the range [-14 mm : 10 mm], though lower surface values may be observed on the rim. The difference at the actuators between the surfaces necessary to illuminate all three coverages is contained in the interval [-13 mm : 12 mm].

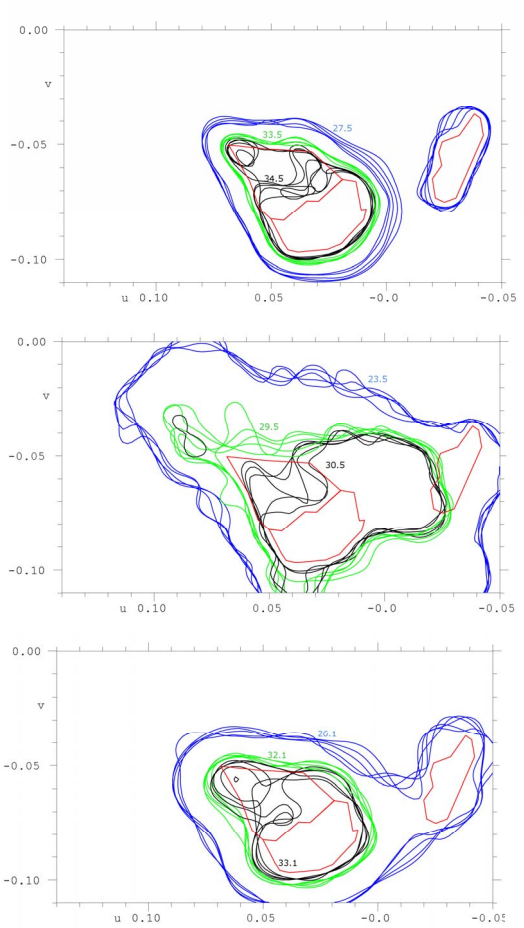

Fig. 5 Polygons for the coverage $C_1+C_2+C_3$ (red curve) and amplitude of the co-polar component (minimum levels) of the obtained far-field in dBi in the satellite CS: case 1 on top, case 2 in the middle, case 3 below.

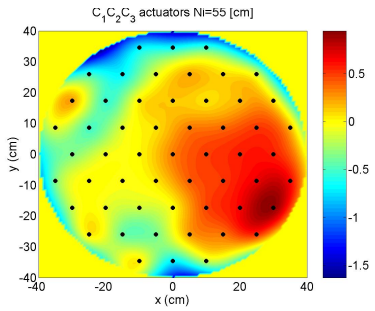

Fig. 6 Subreflector shaping relative to the parent ellipsoid obtained for Case 3 with 55 actuators, for the coverage $C_1+C_2+C_3$.

It was finally computed that by increasing the number of actuators to 130, see Fig. 4, directivities could improve by 0.7 dB over B_1+B_2 but only 0.1 dB over C_1+C_2+C_3 and D_1+D_2.

V. SENSITIVITY ANALYSIS

A sensitivity analysis for the reconfigurable surface made by the interwoven wire mesh with actuators used in Case 3 was then performed.

A. General Sensitivity Analysis

With the purpose of modelling both the inaccuracy of the actuator positioners and possible thermo-elastic distortions, a random error uniformly distributed between [-0.1 mm, 0.1 mm] was added to the *z*-coordinates of the 55 actuators. From these new sets of actuators, the corresponding far-fields over the coverages were computed. For every coverage, 1000 different actuator errors were considered. Mean value and standard deviation of the maximum directivity loss relative to the directivity values reported in TABLE III for Case 3 and observed over the 100% of the coverages are reported in TABLE IV. The corresponding plot of the maximum directivity loss obtained for the 1000 cases is given in Fig. 7 for the coverage C_1+C_2+C_3.

TABLE IV
MEAN VALUE AND STANDARD DEVIATION OF THE MAXIMUM DIRECTIVITY LOSS OVER 100% OF THE COVERAGES, RELATIVE TO TABLE III AND CASE 3.

	B_1B_2	$C_1C_2C_3$	D_1D_2
Mean value μ [dB]	0.2781	0.1964	0.1009
Standard deviation σ [dB]	0.0972	0.0690	0.0558
$\mu+\sigma$ [dB]	0.3753	0.2654	0.1567
$\mu+3\sigma$ [dB]	0.5697	0.4034	0.2683

It is seen that mean value and standard deviation of the maximum directivity loss are related to the size of the coverage.

It was noticed however that the value of the loss reported for example in Fig. 7 only affected a very limited number of stations over the coverages.

Moreover, it was observed that the stations mostly affected by the loss where all located at the border of the coverage, or in the area defined by the beam pointing error, and in most cases existed only for some frequencies.

It was then decided to remove the 1% of the worst stations to obtain the maximum directivity loss, always relative to the results of TABLE III for Case 3, over 99% of the coverages. The corresponding mean values and standard deviations are shown in TABLE V. It is seen that the mean of the maximum directivity losses over 99% of the coverages is less than half of the values reported in TABLE IV for B_1+B_2 and C_1+C_2+C_3 and less than a fourth for D_1+D_2.

TABLE V
MEAN VALUE AND STANDARD DEVIATION OF THE MAXIMUM DIRECTIVITY LOSS OVER 99% OF THE COVERAGES, RELATIVE TO TABLE III AND CASE 3.

	B_1B_2	$C_1C_2C_3$	D_1D_2
Mean value μ [dB]	0.1177	0.0973	0.0232
Standard deviation σ [dB]	0.0607	0.0435	0.0616

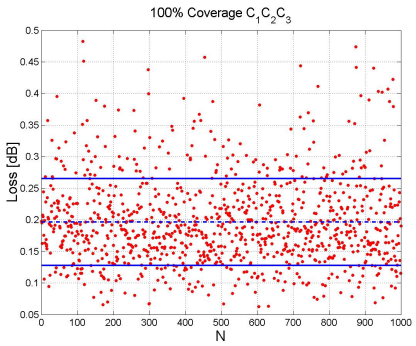

Fig. 7 Maximum directivity loss on 100% of C_1+C_2+C_3 for 1000 different cases: mean value (dashed line) and mean value±standard deviation (continuous line).

B. Actuator free

It was then decided to study the effect given by an actuator which is free to move. By removing the failing actuator from the set of the known actuators necessary for a given coverage, the new subreflector surface was computed and the effect on the radiated field was analysed. It was found that the actuator on which the largest force was applied [3] provided, when removed, the largest directivity loss and was thus the most critical one, see Fig. 8 on the left. It was seen that directivities decreased by 1.17 dB over the coverage B_1+B_2, 1.13 dB over the coverage C_1+C_2+C_3 and 0.27 dB over D_1+D_2 relative to the nominal values reported in TABLE III for Case 3.

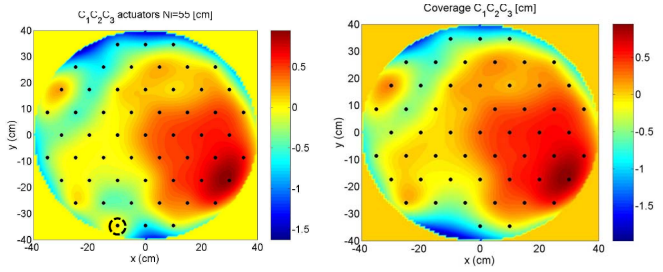

Fig. 8 Subreflector shaping relative to the parent ellipsoid for the coverage C_1+C_2+C_3 and actuator with the largest force highlighted (on the left). On the right, optimized shaping given by the remaining 54 actuators.

To study the capability of the reconfigurable surface of compensating for a free actuator, a new POS5 optimization was performed on the remaining 54 actuators. The optimization on the remaining 54 actuators showed that on each coverage it was possible to re-obtain the same directivity values reported in TABLE III for Case 3. The new subreflector surface obtained by the remaining 54 actuators is shown in Fig. 8 on the right: the surface is very similar to the original on the left, though an actuator is now missing.

C. Actuator stuck

The effect of an actuator that was stuck at a certain *z*-position, and thus could not be reconfigured, was then modelled. For the coverage C_1+C_2+C_3, all control points were set to the expected *z*-values while the one that exhibited the largest *z*-variation in changing from the coverage B_1+B_2 was kept fixed. The new subreflector surface was thus computed and its effect on the radiated field was analysed. On the basis

of the distance relative to the subreflector rim and the actuators z-variation in changing from B_1+B_2 to $C_1+C_2+C_3$ (see Fig. 9), four cases were taken into account, one at a time.

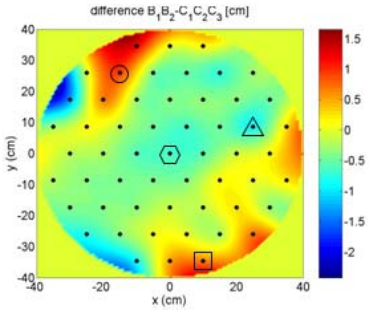

Fig. 9 Difference between the subreflector shaping for the coverage B_1+B_2 and $C_1+C_2+C_3$ and the considered stuck actuators.

It was seen that the sign of the actuator z-difference was irrelevant but that its absolute value and the distance of the actuator from the rim were important. In particular, a stuck actuator which is located on or close to the rim (square, circle and triangle in Fig. 9) has a smaller effect (loss from 0.43 dB to 1.99 dB) on the antenna performances than one located at the center of the subreflector (hexagon in Fig. 9), for which the loss becomes 11.01 dB, relative to TABLE III and Case 3.

The z-coordinate of the stuck actuator given by the circle (x_o= -15.2 cm, y_o=25.6 cm) which provided a loss of 1.99 dB was then used as a constraint for a new optimization over the remaining 54 actuators, to study the capability of the reconfigurable surface to compensate for the actuator failure. In this case, the subreflector shaping was modelled by splines (12x12) instead of by actuators, to use an option on subreflector constraints already implemented and tested in POS5. It is recalled that the directivity over the coverage $C_1+C_2+C_3$ given by 55 actuators is equal to the one provided by 12x12 splines. The subreflector surface was thus re-optimized to illuminate the coverage $C_1+C_2+C_3$ with the constraint that at the point x_oy_o the surface passed through z_o=-74.05 cm (ellipsoid+shaping relative to the $x_{sub}y_{sub}$-coordinate system), in accordance to the value given by the surface shaped to B_1+B_2. The original subreflector surface shaped to $C_1+C_2+C_3$ passed through z_c=-74.68 cm (relative to the $x_{sub}y_{sub}$-coordinate system), and this gave thus rise to a difference d=0.63 cm at x_oy_o. The new optimization provided the same directivity values of TABLE III for Case 3: the new surface passed through $x_oy_oz_o$ and was almost identical to the original $C_1+C_2+C_3$ surface translated by d, see Fig. 10. It was seen that, though the shaping of the new subreflector increased everywhere by 0.63 cm, XPD performances changed only very slightly when compared to the original, meaning that the compensated geometry was thus maintained.
It was finally decided to perform a new optimization with the additional constraint that the shaping relative to the ellipsoid should be confined to the interval [-1cm : 1cm], in order to model the limited stroke of the actuators. A loss of 0.7 dB was obtained. The corresponding subreflector shaping is shown in Fig. 11.

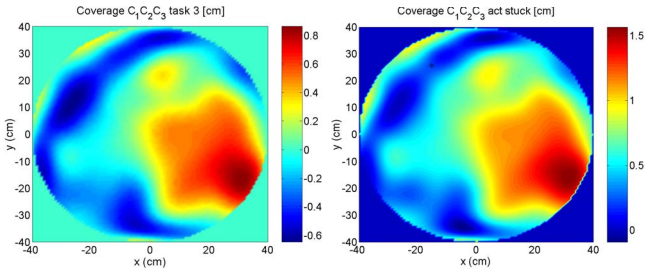

Fig. 10 Shaped subreflector surface with 12x12 splines relative to the parent ellipsoid in cm for the coverage $C_1+C_2+C_3$: on the left the original, on the right the one obtained for a stuck actuator at $x_oy_oz_o$.

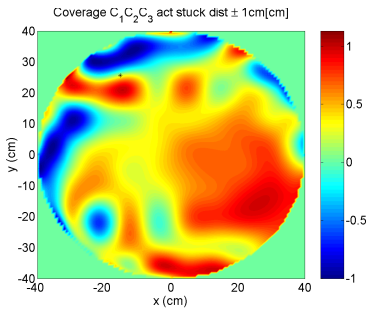

Fig. 11 Shaped subreflector surface with 12x12 splines relative to the parent ellipsoid in cm for the coverage $C_1+C_2+C_3$: stuck actuator at $x_oy_oz_o$ and ±1cm constraint.

VI. CONCLUSIONS

A feasibility study and sensitivity analysis for a reconfigurable dual reflector antenna in Ku band was performed. It was shown that the use of a reconfigurable subreflector together with a fixed shaped main reflector could improve the directivity over the coverages up to 2.9 dB relative to the traditional performances given by a reflector shaped for the envelope of the coverages. The reconfigurable subreflector was modelled as a mesh of interwoven wires supported by 55 actuators. It was found that a random error of ±0.1mm over the 55 actuators provided a directivity loss of mean value equal to 0.11 dB over 99% of the largest coverage, but only of 0.09 dB and 0.02 dB over the 99% of the smaller coverages. It was also shown that though a free actuator could give a directivity loss up to 1.17 dB in the worst case, the remaining 54 actuators could successfully compensate for the failure with a new shaping. It was then observed that a stuck actuator located on the rim had a smaller effect on the antenna performances than one located at the center of the subreflector.

REFERENCES

[1] K. Pontoppidan, "Reconfigurable reflector surfaces with imparted bending stiffness," TICRA, Denmark,Tech. Rep. *S-582-02,* September 1994.

[2] R. B. Brown, P. K. B. Clarricoats, Z. I. Hai, "The performance of a prototype reconfigurabæe mesh reflector for spacecraft antenna applications," in *Proc. Europ. Microwave Conference,* 1999.

[3] K. Pontoppidan, "Light weight reconformable reflector antenna dish," in *Proc. of the 28th ESA Antenna Workshop on Space Antenna Systems and Technologies,* Noordwijk, The Netherlands, June 2005.

[4] (2008) The POS5 software. [Online]. Available: http://www.ticra.com/script/site/page.asp?artid=6&cat_id=38.